Isolation of Bacteria from Old Corrugated Container Slime and Characterization of their Biofilm-forming Properties

Hua Chen,[a,b,c] Rendang Yang,[a,b] Jianhua Wang,[c,*] Huifang Zhao,[a] Bin Wang,[b] Qizhong Wo,[d] and Bingbing Zheng [a]

With the continuously increasing demand for paper and cardboard products, there is growing concern about the bacteria of the papermaking process. Bacterial growth not only affects normal manufacturing, but it also results in paper products with a total number of bacteria that exceeds the acceptable range, and thus poses a risk to the health of consumers. In this study, 99 pure bacterial strains were isolated from old corrugated containers (OCC) slime. The morphological, physiological, and biochemical properties of the bacterial strains were examined. Furthermore, the isolated strains were tested for their ability to form biofilms. The strains that could form biofilms were identified using 16S rDNA sequencing. The results revealed that some bacteria could form both a biofilm that adhered to the smooth tube wall, as well as abundant flocs at the bottom of the test tube. Conversely, the other bacteria could not form a noticeable biofilm. The bacteria with the most powerful biofilm-forming ability were identified as *Proteus penneri*, *Klebsiella variicola*, *Klebsiella* sp., and *Proteus mirabilis*.

Keywords: Bacteria; OCC pulp; Biofilm-forming; Papermaking

Contact information: a: Zhejiang Provincial Collaborative Innovation Center of Agricultural Biological Resources Biochemical Manufacturing, Zhejiang Provincial Key Lab for Chem. & Bio. Processing Technology of Farm Product, Key Laboratory of Recycling and Eco-treatment of Waste Biomass of Zhejiang Province, Zhejiang University of Science and Technology, 310023, Hangzhou, China; b: State Key Lab of Pulp and Paper Engineering, South China University of Technology, 510640, Guangzhou, China; c: Zhejiang Yongtai Paper Co. Ltd., 311421, Hangzhou, China; d: Food Quality and Safety Inspection and Testing Center of Hangzhou Fuyang, 311421, Hangzhou, China;
**Corresponding author: keji@yongtaipaper.com*

INTRODUCTION

With the rapid development of the modern pulp and paper industry, the shortage of fibrous raw material has become increasingly problematic. However, the use of waste paper has remarkably increased to alleviate this problem. According to the annual report of China's paper industry in 2015 that was released by China Paper Association, the use of waste paper fiber in the Chinese paper industry reached 65% in 2015 (CPA 2015).

To reduce the costs and improve downstream properties, such as printing, various fillers are added to pulp, including calcium carbonate, talc, carbon dioxide, and china clay (Chen *et al*. 2015; Rantanen *et al*. 2015; Chen *et al*. 2016; Li *et al*. 2016b). The addition of such materials usually reduces the quality of the waste paper fiber, mainly because these fillers hinder hydrogen bonding between the fibers. Another important factor leading to a reduction in waste paper fiber quality is 'hornification'. This property is characterized by changes in the fiber morphology, physical properties, chemical composition, and fiber

surface conditions that results in the reduction of the porosity of the waste paper fiber. The mechanisms involved in hornification include reorganization of the cell walls, irreversible closure of pores, and hemicellulose-polyxylose interactions (Chen *et al*. 2015; Hettegger *et al*. 2016; Pèlach *et al*. 2016). To compensate for these problems, a large amount of high-molecular weight polymer is added to the pulp to increase hydrogen bonding between the fibers (Ashori *et al*. 2013; Fan *et al*. 2015; Li *et al*. 2016a). Of these polymers, starch has the advantages of being biodegradable, environmentally friendly, renewable, and it can be sourced from a wide range of products. As a result, starch has been widely used as a paper enhancer.

However, the glucose generated after starch hydrolysis in pulp provides bacteria with a good nutrient source. This, along with the increasingly prominent use of recycled water because of environmental stress, causes a rapid growth and proliferation of microorganisms, such as bacteria and fungi. When biofilms form and then detach during the manufacturing process, contamination of the equipment and blockage of the water-removal devices, such as the forming fabric and wet-press felts, can occur. Over time, this produces low-quality paper, affects the normal operation of the machinery, and leads to a reduction in the paper product quality and printing machine efficiency. One of the most effective ways to inhibit blockage of the process is to reinforce pipeline cleaning, but this process will also cause the enhancement of discharge, resulting in rising production costs.

To solve the problem of slime, various biocides are used, such as isothiazolinone (CIT/MIT) (Lin *et al*. 2010) and phenolic compounds (Neyret *et al*. 2014). Recently, antibacterial proteins (Barbiroli *et al*. 2012) and ciprofloxacin (CipHCl) (Dong *et al*. 2014) have also been proposed for antibacterial applications. However, most of the microorganisms in slime have thick, viscous capsules that are resistant to biocides by up to 1000 times that of ordinary plankton. Furthermore, bacteria can attach firmly to the surface of pipelines *via* the capsule, which makes them resistant to washing and encourages proliferation (Wang 2000). Over recent decades, many species of bacteria have been found in slime. Factors such as different bacterial species, different bacterial carriers, and organic substances can influence the germicidal efficacy of different biocides. Thus, the identification of the microorganisms in slime is particularly important for the selection of suitable biocides.

EXPERIMENTAL

Materials

Sample collection

Slime was collected from the wire section of PM 7 paper machine of Zhejiang Yongtai Paper Co. Ltd. (Hangzhou, China). The main raw pulp material from the paper machine was old corrugated container (OCC) waste paper. The solids concentration of the slime was 4.63%. The content of cellulose, hemicellulose, and lignin of fiber was respectively 60.82%, 9.38%, and 5.54%.The slime was placed in a sealed and disinfected bag, transported to lab in an hour at 20 °C, and then stored at 4 °C for 2 days.

Main experimental reagents

The main experimental reagents were 2xPCR Mix (Dongsheng Biotech Co., Ltd., Guangzhou, China), agarose (GenStar Biosolutions Co., Ltd., Beijing, China), DNA markers (Takara Biotechnology Co., Ltd., Dalian, China), glutaraldehyde solution (Xilong

Scientific Co., Ltd., Shantou, China), and a HBI microbial biochemical identification kit (Hope Bio-technology Co., Ltd., Qingdao, China).

Methods

The equipment used in this study were a polymerase chain reaction (PCR) machine (T-Gradient, Biometra, Göttingen, Germany), scanning electron microscope (SEM) (JSM-6360LA, Jeol Ltd., Tokyo, Japan), and 3.2 million-pixel integrated digital microscope (SMARTe-320, Optec Instrument Co., Ltd., Chongqing, China).

Isolation and purification of the microorganisms

At an aseptic operating station, a small amount of freshly-sampled slime was removed using a sterile inoculation needle and streak-plated on a solid medium in a Z-shape. Ten plates were streaked for each of the four mediums used in this study. The 40 plates were then incubated at room temperature (25 °C) for 2 d. Colonies with different morphologies were progressively isolated and streak-plated until pure bacteria clones were obtained.

After isolation and purification, 99 pure isolates were obtained from the fresh slime samples. The isolates were then successfully cultured in the JLJ (n = 19), KB (n = 22), LB (n = 28), and NYGA (n = 30) media.

For the JLJ medium, 10 g of peptone, 0.5 g of NaCl, 0.5 g of K_2PO_4, 0.5 g of $MgSO_4 \cdot 7H_2O$, and a trace amount of $Fe_2(SO_4)_3 \cdot 7H_2O$ were dissolved in an inlet pulp sample (1000 mL; filter sterilized) and divided into 10 flasks (100 mL each). Agar powder (1.7 g) was added to each bottle and sterilized at 120 °C for 16 min.

For the KB medium, 20 g of peptone, 1.5 g of K_2PO_4, and 1.5 g of $MgSO_4 \cdot 7H_2O$ were dissolved in deionized water (1000 mL). The pH was adjusted to 7.2, and then the solution was divided into 10 flasks (100 mL each). Agar powder (1.7 g) was added to each bottle and sterilized at 120 °C for 16 min.

For the LB medium, 10 g of peptone, 5 g of yeast extract, and 10 g of NaCl were dissolved in deionized water (1000 mL) and divided into 10 flasks (100 mL each). Agar powder (1.7 g) was added to each bottle and sterilized at 120 °C for 16 min.

For the NYGA medium, 3 g of yeast extract, 5 g of beef extract, and 20 g of sucrose were dissolved in deionized water (1000 mL). The pH was adjusted to 7.0, and then the solution was divided into 10 flasks (100 mL each). Agar powder (1.7 g) was added to each bottle and sterilized at 120 °C for 16 min.

Examination of the biofilm-forming ability

At a sterile operating station, pure colonies were picked using sterilized toothpicks. The colonies were inoculated into the liquid LB culture medium and incubated at 37 °C on a shaker (150 rpm) for 48 h. The ability of the isolate to form a biofilm on the wall of the test tube was then studied.

16S rDNA identification of the biofilm-forming bacteria

16S rDNA of each isolate was amplified by using 27F and 1492R as the PCR primers. The universal primer 27F was 5'-AGAGTTTGATCMTGGCTCAG-3', and the universal primer 1492R was 5'-GGTTACCTTGTTACGACTT-3'. The PCR reaction system (50 μL) consisted of 25 μL of 2xPCR Mix, 19 μL of double distilled water (ddH_2O), 2 μL of DNA template, 2 μL of forward primer (10 μmol/L), and 2 μL of reverse primer (10 μmol/L). The PCR amplification conditions used were 94 °C for 4 min, 94 °C for 30 s,

55 °C for 30 s, 72 °C for 2 min, 30 cycles, and 72 °C for 10 min. The PCR products were then sequenced and compared by BLAST on NCBI (Bethesda MD, USA). The phylogenetic tree was constructed by MEGA 6.0 software (Temple University, Philadelphia, PA, USA).

Grams staining

A small water droplet was placed on the slide for smearing. A small bacterial colony was picked using an inoculation loop and suspended in the water droplet. The water was allowed to evaporate at room temperature before the slide underwent flame fixation.

During the initial staining, the samples were stained in an ammonium oxalate crystal violet staining solution for 1 to 2 min. Next, the slide was washed by allowing tap water to flow from the top of the slide downwards until it was colorless.

The samples then underwent mordanting. The samples were stained with Gram's iodine dye solution for 1 to 3 min, and then were washed with water.

The samples were dehydrated. Alcohol decolorization was performed for 30 to 60 s, which was followed by a wash with water.

Counterstaining was then performed, where the samples were stained with red carbonic acid for 10 to 20 s, and were then washed with water.

Microscopic examination was then conducted. Once the samples were completely dry at 32 °C, the specimen was first examined under low-power magnification, and then by high-power magnification and oil immersion.

Spore staining

Bacillus spp. and *Bacillus subtilis*, which were cultured for approximately 24 h, were smeared, dried, and fixed to slides. Three to five drops of malachite green dye were added to the fixed smear. The slides were held with a wooden clip and flame-heated until the dye steamed, but did not boil. Each slide was then further heated for another 4 to 5 min. Evaporation of the dye must be avoided, and as such, small amounts of dye were added as necessary. A 10-min incubation in saturated malachite green solution could also have been used in lieu of the heating step. The excess dye solution was allowed to drip off the slide. The samples were then washed with water until the malachite green no longer faded after the glass cooled. A counterstain with a safranin solution was performed for 1 min, and then the sample was rinsed with water. The samples were examined by oil immersion after they were completely dry.

Capsule staining

The standard bacterial collection and smearing procedures were followed. The samples were naturally dried in air for fixation. Heat-drying for fixation was avoided. Staining was achieved by incubating the smear in a 1% crystal violet aqueous solution for 2 min. The samples were rinsed with 20% copper sulfate aqueous solution and blot-dried with absorbent papers to achieve decolorization. For the microscopic examination, examination by oil immersion was conducted after the specimens were dry.

Physio-biochemical identification

The HBI Microbial Biochemical Identification System (Hope Bio-technology Co., Ltd., Qingdao, China) was used for the physio-biochemical identification of the bacterial isolates. This system contained a 20-well biochemical identification strip and an oxidase test strip. The reagents contained in each well were ortho-nitrophenyl-β-galactoside

(ONPG), arginine (ADH), lysine (LDH), ornithine (ODC), citrate (CIT), hydrogen sulfide (H_2S), urease (URE), lactose (LAC), indole (IND), VP, gelatin (GEL), glucose (GLU), mannitol (MAN), inositol (INO), sorbitol (SOR), rhamnose (RHA), sucrose (SAC), melibiose (MEL), amygdalin (AMY), arabinose (ARA), and oxidase (OX).

A biochemical identification strip was taken from the package, and the lid was opened. Holes were made using a punching device. If any of the reagents appeared stained or discolored, the strip was discarded and a new one was used. Using an inoculation loop, a single colony was picked from a prepared nutrient agar or tryptone soya agar plate and inoculated into sterile saline (2 mL), which was then thoroughly ground and mixed in a mixer to prepare the bacteria suspension. Using a pipette, 100 µL of the bacteria suspension was added into each hole of the biochemical identification strip. The ADH, LDH, and ODC holes were covered with 200 µL to 300 µL of sterile liquid paraffin. The biochemical identification strip was then covered and placed onto a plastic base. The reaction was incubated at 35 °C to 37 °C for 18 h to 24 h. An additional 18 h to 24 h incubation was performed if a negative result was observed for the gelatin biochemical reaction. Before observing the results, the test strip was incubated at 2 °C to 8 °C. The oxidase test strip was taken out of the light-shielding paper and 100 µL of 0.85% NaCl solution was transferred to one end of the paper strip using a pipette. A single bacterial colony was then smeared onto the wet paper strip. The results were recorded after 60 s.

Scanning electron microscopy

For the slide treatment, coverslips (1 cm^2) were prepared by soaking them overnight with 1 M HCl, which was followed by several rinses with anhydrous ethanol and sonication for 30 min (300 W, 3 s sonication followed by a 3-s pause). The prepared coverslips were then placed in a clean petri dish and oven-dried for future use.

The 0.2 M PBS solution (pH 7.4) consisted of 2.6 g of sodium dihydrogen phosphate ($NaH_2PO_4 \cdot H_2O$) and 29 g of disodium hydrogen phosphate ($Na_2HPO_4 \cdot 12H_2O$) dissolved in 500 mL of double distilled water.

One liter of sterile water and a sterilized round bottomed flask were prepared for further use. For the 2.5% glutaraldehyde solution, 25% glutaraldehyde, sterile water, and 0.2 M PBS solution were mixed at a ratio of 1:4:5.

By dilution with sterile water, 30%, 50%, 70%, 80%, 90%, and 100% alcohol solutions were prepared.

For the bacterial treatment and fixation, the bacteria were sampled while in the logarithmic phase. A 1 mL sample was removed from the culture medium and centrifuged at 8000 rpm at room temperature for 1 min. The supernatant was discarded and 2.5% glutaraldehyde was added to the pellet, which was followed by thorough mixing and fixation overnight at 4 °C.

Gradient dehydration using ethanol was then performed. The fixed bacteria were centrifuged at 8000 rpm for 1 min and the supernatant was removed. They were then washed three times with PBS and dehydrated in increasing amounts of ethanol (30%, 50%, 70%, 80%, and 90%). The samples were allowed to stand for 15 min after each ethanol addition, which was followed by centrifugation at 8000 rpm for 1 min. Next, 100% ethanol washes were performed in duplicate under the aforementioned conditions. Finally, the sample was re-suspended in approximately 300 µL to 600 µL of anhydrous ethanol and stored until future use.

Double-sided adhesive was attached to a large clean petri dish and marked accordingly. Coverslip pieces were transferred onto the double-sided adhesive with flat

head tweezers. Three coverslips were usually prepared for each sample. Bacterial suspensions (7 µL to 10 µL) were aliquoted onto each coverslip surface, which was then oven-dried with the dish covered in plastic wrap. Finally, the samples were examined under a microscope.

RESULTS AND DISCUSSION

Isolation and Purification of the Bacteria

The colony morphology was mainly observed as round with a neat edge and central protrusion (Table 1). The majority of the colonies had a milky white color. The LB7 and LB11 colonies displayed special morphologies, which were yurt- and petal-like, respectively.

Biofilm-forming Ability

The results showed that among the 99 pure bacterial strains that were cultured, 18 possessed the ability to form biofilms (Fig. 1). The isolates that showed the strongest biofilm-forming ability were KB3, LB18, LB24, NYGA5, NYGA9, and NYGA15. Large amounts of bacterial flocs were observed at the bottom of the KB6, LB24, and NYGA3 tubes.

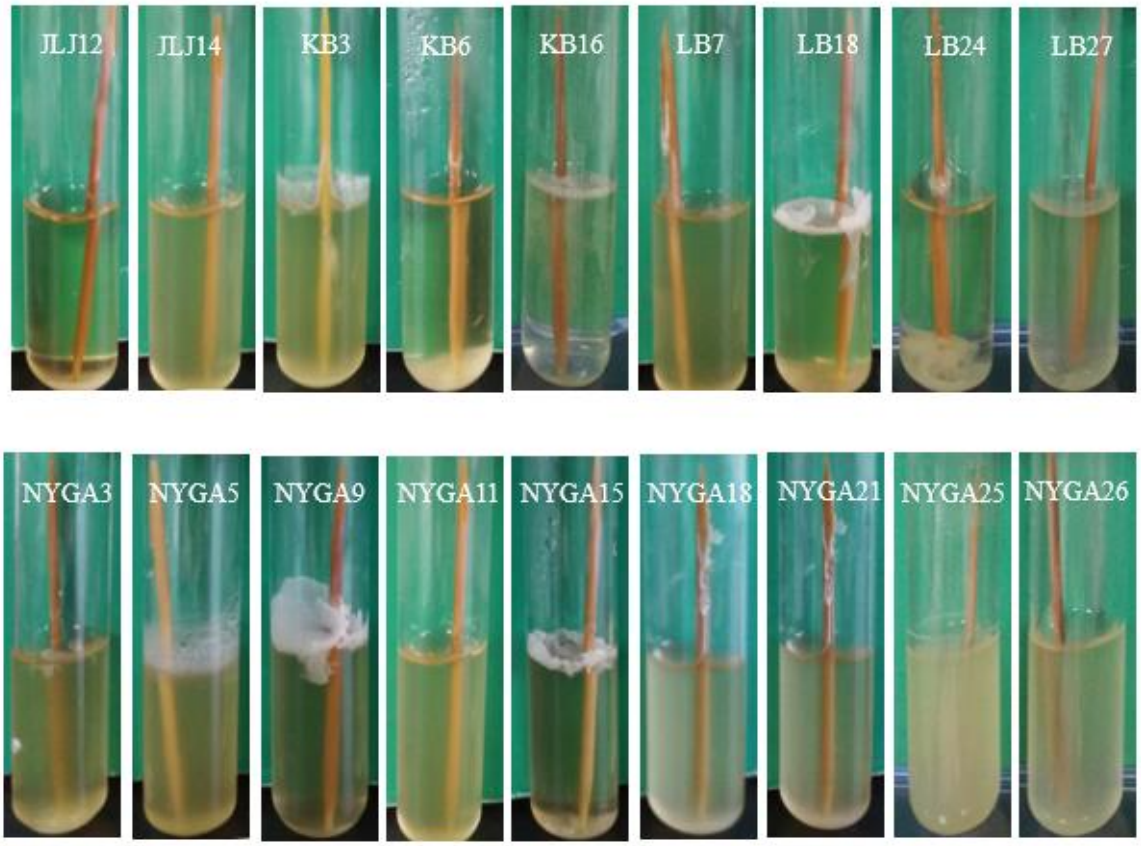

Fig. 1. Biofilm-forming ability test

Table 1. Bacterial Colony Morphology and Biofilm-forming Ability Statistics

Medium and Code	Colony Morphology	Diameter	Edge	Protrusion	Color	Surface Texture	Transparency	Biofilm Formation
JLJ1	Round	1.5 mm	Neat	Central protrusion	Burgundy	Smooth and moist	Opaque	-
JLJ2	Round	1.5 mm	Neat	Central protrusion	Milky white	Smooth and moist	Opaque	-
JLJ3	Round	1.0 mm	Neat	Central protrusion	Milky yellow	Smooth and moist	Opaque	-
JLJ4	Round	4.0 mm	Neat	Central protrusion	Milky white	Smooth and moist	Opaque	-
JLJ5	Round	1.5 mm	Neat	Central protrusion	Milky white	Smooth and moist	Translucent	-
JLJ6	Round	1.5 mm	Neat	Central protrusion	Milky yellow (slightly)	Smooth and moist	Opaque	-
JLJ7	Round	0.2 mm	Neat	Central protrusion	Milky white	Smooth and moist	Opaque	-
JLJ8	Round	1.5 mm	Neat	Empty middle	Burgundy	Smooth and moist	Opaque	-
JLJ9	Round	2.0 mm	Neat	Middle concave	Milky white	Smooth and moist	Opaque	-
JLJ10	Irregular	3.0 mm	Not neat	Middle concave	Milky white	Dry	Opaque	-
JLJ11	Irregular	3.5 mm	Not neat	Middle convex	Milky white	Dry wrinkles	Opaque	-
JLJ12	Oval	4.0 mm	Neat	Flat	Milky white	Smooth and moist	Opaque	+
JLJ13	Round	1.5 mm	Neat	Central protrusion	Milky white	Smooth and moist	Opaque	-
JLJ14	Irregular	2.0 mm	Neat	Flat	Milky yellow	Dry wrinkles	Opaque	+
JLJ15	Round	3.0 mm	Neat	Central protrusion	Milky white	Dry wrinkles	Opaque	-
JLJ16	Round	1.5 mm	Neat	Flat	Milky yellow	Smooth and moist	Opaque	-

Medium and Code	Colony Morphology	Diameter	Edge	Protrusion	Color	Surface Texture	Transparency	Biofilm Formation
JLJ17	Round	0.5 mm	Neat	Central protrusion	Milky white	Smooth and moist	Opaque	-
JLJ18	Round	2.0 mm	Neat	Central protrusion	Yellow (with a transparent edge)	Smooth and moist	Opaque	-
JLJ19	Round	1.0 mm	Neat	Central protrusion	Milky white	Smooth and moist	Opaque	-
KB1	Irregular	2.5 mm	Not neat	Central protrusion	Milky white	Smooth and moist	No	-
KB2	Round	3 mm	Neat	Central protrusion	Milky white	Smooth and moist	No	-
KB3	Round	2.5 mm	Neat	Central protrusion	Yellowish-green	Smooth and moist	No	++
KB4	Round	2 mm	Neat	Central protrusion	Milky white	Smooth and moist	No	-
KB5	Irregular	2.5 mm	Not neat	Central protrusion	Milky white	Smooth and moist	No	-
KB6	Round	3 mm	Neat	Flat	Milky white	Half dry	No	+
KB7	Irregular	2 mm	Neat	Flat	Red	Smooth and moist	No	-
KB8	Round	3 mm	Not neat	Flat	Milky white	Half dry	No	-
KB9	Flower-like	2 mm	Not neat	Flat	Milky white	Half dry	No	-
KB10	Round	3 mm	Neat	Central protrusion	Milky white	Smooth and moist	Translucent	-
KB11	Round	2 mm	Neat	Central protrusion	Milky white	Smooth and moist	No	-
KB12	Round	0.8 mm	Neat	Central protrusion	White	Smooth and moist	No	-
KB13	Round	1 mm	Neat	Central protrusion	Pale yellow	Smooth and moist	No	-
KB14	Round	0.8 mm	Neat	Central protrusion	Milky white	Smooth and moist	No	-

Medium and Code	Colony Morphology	Diameter	Edge	Protrusion	Color	Surface Texture	Transparency	Biofilm Formation
KB15	Round	0.7 mm	Neat	Central protrusion	Yellow	Smooth and moist	No	-
KB16	Irregular	1.5 × 0.8 cm	Not neat	Multiple small protrusions	White	Smooth and moist	No	+
KB17	Round	1.5 mm	Neat	Central protrusion	Yellowish-green	Smooth and moist	No	-
KB18	Round	1 mm	Neat	Central protrusion	Milky white	Smooth and moist	No	-
KB19	Round	5 mm	Neat	Slightly concave	Pale yellow	Smooth and moist	No	-
KB20	Irregular	0.5 mm	Petal-like	Flat	Milky white	Smooth and moist	No	-
KB21	Round	8 mm	Neat	Flat	White	Smooth and moist	Yes	-
KB22	Round	1.5 mm	Neat	Central protrusion	Colorless	Smooth and moist	Yes	-
LB1	Round	2.0 mm	Neat	Central protrusion	Milky white	Smooth and moist	Opaque	-
LB2	Round	2.0 mm	Neat	Central protrusion	Milky yellow	Smooth and moist	Translucent	-
LB3	Irregular	3.0 mm	Not neat	Central protrusion	Milky yellow (slightly)	Dry wrinkles	Opaque	-
LB4	Round	0.2 mm	Neat	Central protrusion	Dark yellow	Smooth and moist	Opaque	-
LB5	Round	4.0 mm	Neat	Flat	Milky white	Smooth and moist	Opaque	-
LB6	Round	2.5 mm	Neat	Flat	Milky white	Smooth and moist	Translucent	-
LB7	Yurt-like	2.5 mm	Neat	Yurt-like protrusion	White	Protrusion was covered by a thin film	Opaque	+

Medium and Code	Colony Morphology	Diameter	Edge	Protrusion	Color	Surface Texture	Transparency	Biofilm Formation
LB8	Irregular	3.0 mm	Not neat	Central protrusion	Milky white	Smooth and moist	Opaque	-
LB9	Round	3.0 mm	Neat	Middle white spots surrounded by dry wrinkles	Milky white	Half dry with wrinkles	Opaque	-
LB10	Round	2.0 mm	Neat	Central protrusion	Burgundy (darker middle with a lighter periphery)	Smooth and moist	Opaque	-
LB11	Irregular (Flower-like)	2.5 mm	Not neat	Flat	Milky yellow	Dry wrinkles	Opaque	-
LB12	Round	3.0 mm	Neat	Central protrusion	Milky yellow	Smooth and moist	Opaque	-
LB13	Round	2.0 mm	Neat	Flat	Milky white	Half Dry	Transparent	-
LB14	Round	5.0 mm	Needle-like	Central protrusion	Milky yellow	Dry wrinkles	Opaque	-
LB15	Round	1.0 mm	Neat	Central protrusion	Burgundy	Smooth and moist	Opaque	-
LB16	Irregular	3.0 mm	Neat	Central protrusion	Milky white	Smooth and moist	Opaque	-
LB17	Round	2.0 mm	Neat	Central protrusion	Burgundy	Smooth and moist	Opaque	-
LB18	Round	2.5 mm	Neat	Yurt-like protrusion	White	Protrusion covered by a film	Opaque	+++
LB19	Round	3.0 mm	Neat	Central protrusion	Yellow	Smooth	Opaque	-
LB20	Round	1.0 mm	Neat	Central protrusion	Milky white	Smooth	Opaque	-
LB21	Round	1.0 mm	Neat	Central protrusion	Milky white	Smooth	Opaque	-

Medium and Code	Colony Morphology	Diameter	Edge	Protrusion	Color	Surface Texture	Transparency	Biofilm Formation
LB22	Round	5.0 mm	Not neat	No protrusion	White	Rough	Transparent	-
LB23	Oval	3.0 mm	Not neat	Central protrusion	Red	Smooth	Opaque	-
LB24	Round	4.0 mm	Not neat	Flat	White	Rough	Opaque	++
LB25	Round	3.0 mm	Not neat	Central protrusion	Milky white	Smooth	Transparent	-
LB26	Round	2.0 mm	Neat	Central protrusion	Milky white	Smooth	Opaque	-
LB27	Round	3.0 mm	Neat	Higher protrusion in middle	White	Smooth	Opaque	+
LB28	Round	0.5 mm	Neat	Central protrusion	Milky white	Smooth	Opaque	-
NYGA1	Round	1 cm	Neat	Central protrusion	Milky white	Smooth and moist	No	-
NYGA2	Round	7 mm	Neat	Central protrusion	Transparent	Smooth and moist	Yes	-
NYGA3	Oval	1.1 × 8 mm	Uneven	Middle convex	White	Dry and rough	No	+
NYGA4	Round	7 mm	Neat	Central protrusion	Transparent	Smooth and moist	Yes	-
NYGA5	Round	4 mm	Neat	Central protrusion	Milky white	Smooth and moist	No	++
NYGA6	Irregular	6 mm	Uneven	Central protrusion	Milky white	Smooth and moist	Slightly transparent	-
NYGA7	Round	3 mm	Neat	Slightly convex	Milky white	Smooth and moist	No	-
NYGA8	Round	3 mm	Neat	Central protrusion	Milky white	Smooth and moist	No	-
NYGA9	Irregular	1.6 × 1.1 cm	Uneven	Central protrusion	Milky white	Smooth and moist	No	+++
NYGA10	Round	1 mm	Neat	Central protrusion	Pink	Smooth and moist	No	-

Medium and Code	Colony Morphology	Diameter	Edge	Protrusion	Color	Surface Texture	Transparency	Biofilm Formation
NYGA11	Round	2 mm	Neat	Central protrusion	Red	Smooth and moist	No	+
NYGA12	Round	3 mm	Neat	Central protrusion	Milky white	Smooth and moist	No	-
NYGA13	Round	4 mm	Neat	Central protrusion	Milky white	Smooth and moist	No	-
NYGA14	Round	7 mm	Neat	Central protrusion	Milky white	Smooth and moist	No	-
NYGA15	Round	1.1 cm	Uneven	Central protrusion	Milky white	Dry and rough	No	+++
NYGA16	Irregular	9 × 2 mm	Uneven	Rugged	Yellow	Dry and rough	No	-
NYGA17	Round	3 mm	Neat	Central protrusion	Yellow	Smooth and moist	No	-
NYGA18	Round	1 cm	Neat	Slightly concave	Milky white	Smooth and moist	No	+
NYGA19	Round	2 mm	Neat	Central protrusion	Yellow	Smooth and moist	No	-
NYGA20	Irregular	1 × 1.3 cm	Not neat	Slightly concave	Milky white	Smooth and moist	No	-
NYGA21	Irregular	2.5 mm	Teeth-like	Central protrusion	Milky white	Smooth and moist	No	+
NYGA22	Round	3 mm	Neat	Central protrusion	Yellow	Smooth and moist	Edge transparent	-
NYGA23	Nil	Smudged 3 cm	Umbrella-like	Flat	Milky white	Half dry	No	-
NYGA24	Round	3.5 mm	Neat	Bubbly	Milky white	Smooth and moist	No	-
NYGA25	Round	2.5 mm	Neat	Central protrusion	Milky yellow	Smooth and moist	No	+
NYGA26	Round	0.5 mm	Neat	Central protrusion	Milky yellow	Smooth and moist	No	+
NYGA27	Round	1 mm	Neat	Central protrusion	Milky white	Smooth and moist	Translucent	-

Medium and Code	Colony Morphology	Diameter	Edge	Protrusion	Color	Surface Texture	Transparency	Biofilm Formation
NYGA28	Round	0.2 mm	Neat	Central protrusion	Milky white	Smooth and moist	No	-
NYGA29	Round	1 mm	Neat	Central protrusion	Milky yellow	Smooth and moist	No	-
NYGA30	Nil	2.5 cm	Tree root distribution	Flat	Milky white	Dry	No	-

Note: biofilm formation: "-" means no biofilm formation ability,"+" means slight biofilm formation ability,"++" means moderate biofilm formation ability, "+++" means strong biofilm formation ability.

16S rDNA Identification of the Biofilm-forming Bacteria

The 18 biofilm-forming bacterial isolates were identified using the 16S rRNA gene. Of the 18 bacterial samples tested, sequencing results were successfully obtained for 14 of the samples (Table 2).

All of the isolates belonged to the phylum *Proteobacteria*. The phylogenetic tree is shown in Fig. 2.

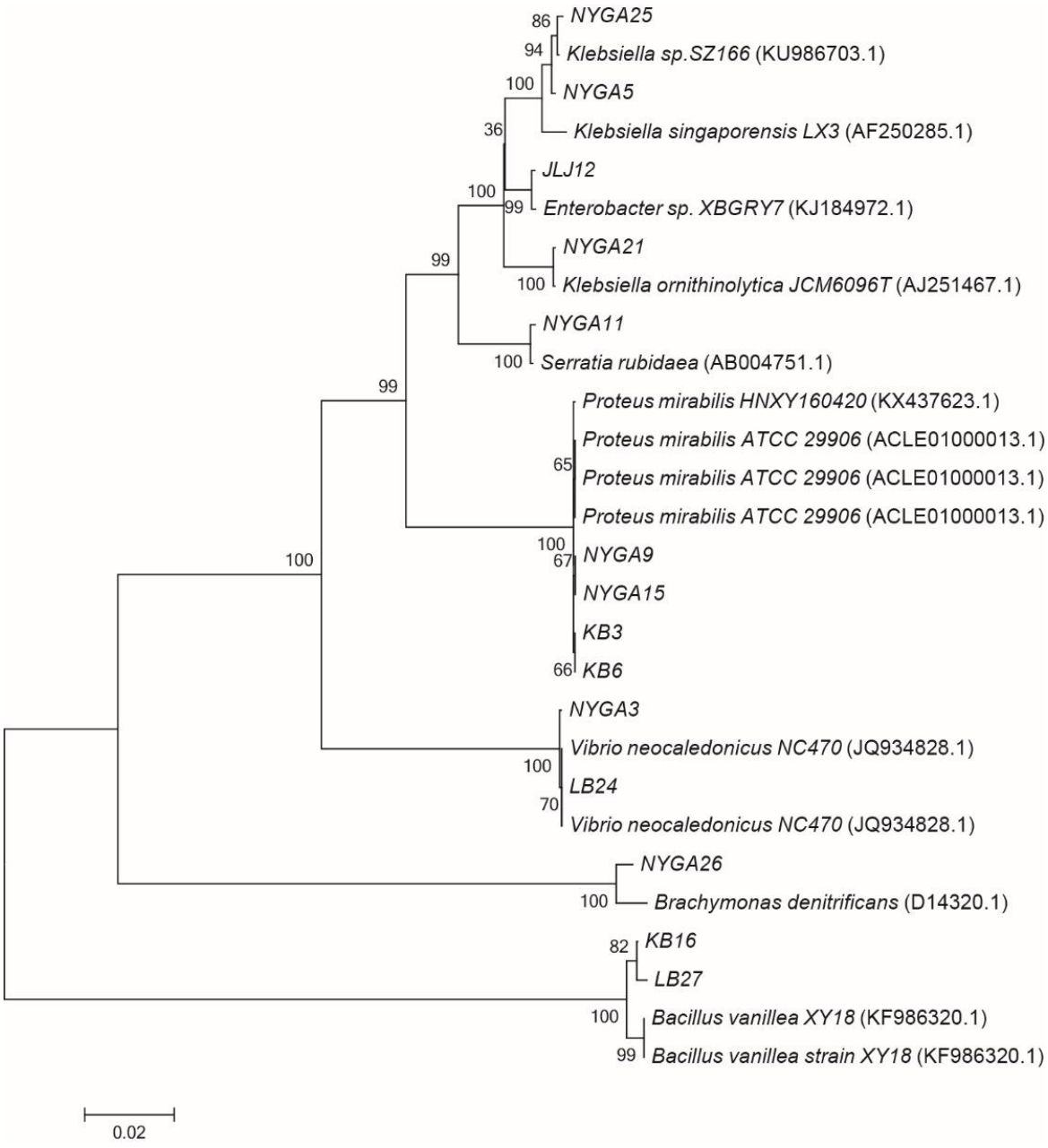

Fig. 2. Phylogenetic tree of the biofilm-forming bacteria

Table 2. 16S rDNA Identification of the Biofilm-forming Bacteria

Strain Code	Comparison Results	Similarity	Classification (Phylum)
JLJ12	*Enterobacter* sp.	99%	*Proteobacteria*
KB3	*Proteus penneri*	99%	*Proteobacteria*
KB6	*Proteus mirabilis*	99%	*Proteobacteria*
KB16	*Bacillus methylotrophicus*	99%	*Proteobacteria*
LB24	*Vibrio neocaledonicus*	99%	*Proteobacteria*
LB27	*Bacillus* sp.	99%	*Proteobacteria*
NYGA3	*Vibrio neocaledonicus*	99%	*Proteobacteria*
NYGA5	*Klebsiella variicola*	99%	*Proteobacteria*
NYGA9	*Klebsiella* sp.	99%	*Proteobacteria*
NYGA11	*Serratia rubidaea*	99%	*Proteobacteria*
NYGA15	*Proteus mirabilis*	99%	*Proteobacteria*
NYGA21	*Raoultella planticola*	99%	*Proteobacteria*
NYGA25	*Klebsiella* sp.	99%	*Proteobacteria*
NYGA26	*Brachymonas denitrificans*	99%	*Proteobacteria*

Gram, Spore, and Capsule Staining

Table 3 shows the results from the gram, spore, and capsule staining of the biofilm-forming bacteria.

Table 3. Staining Results of the Biofilm-forming Bacteria

Strain Code	Bacterial Strain Name	Gram Stain (- negative / + positive)	Capsule Staining (- absent / + present)	Spore Staining (- absent / + present)
JLJ12	*Enterobacter* sp.	-	-	-
KB6	*Proteus mirabilis*	-	-	-
KB16	*Bacillus vanillea*	+	-	+
LB24	*Vibrio neocaledonicus*	-	-	-
LB27	*Bacillus vanillea*	+	-	+
NYGA5	*Klebsiella singaporensis*	-	+	-
NYGA11	*Serratia rubidaea*	-	-	-
NYGA21	*Klebsiella ornithinolytica*	-	-	-
NYGA25	*Klebsiella* sp.	-	+	-
NYGA26	*Brachymonas denitrificans*	-	-	-

Physiological and Biochemical Tests

The results observed for the physiological and biochemical identification tests are shown in Table 4.

Table 4. Physiological and Biochemical Identification Results for the Biofilm-forming Microorganisms

Group	JLJ	KB		LB		NYGA				
Strain Code	12	6	16	24	27	5	11	21	25	26
ONPG	+	+	-	+	+	+	-	+	+	+
Arginine (ADH)	+	+	-	+	-	+	-	+	+	+
Lysine (LDH)	+	+	-	+	+	+	-	+	+	+
Ornithine (ODC)	+	+	+	+	-	+	-	+	+	+
Citric acid (CIT)	+	+	+	+	+	+	+	+	+	-
Hydrogen sulfide (H_2S)	+	+	+	+	-	+	-	+	+	+
Urease (URE)	+	+	+	+	-	+	-	+	+	+
Lactose (LAC)	-	+	-	+	-	-	-	-	+	+
Indole (IND)	+	-	-	-	-	-	-	+	-	+
VP	+	+	-	-	-	+	-	+	+	+
Gelatin (GEL)	+	+	-	+	-	+	+	-	+	+
Glucose (GLU)	-	-	+	-	+	-	+	+	-	-
Mannitol (MAN)	+	+	-	-	+	-	-	+	+	-
Inositol (INO)	-	-	-	+	+	+	-	-	-	+
Sorbitol (SOR)	+	-	-	-	-	-	-	+	-	+
Rhamnose (RHA)	+	+	-	+	-	+	-	+	+	+
Sucrose (SAC)	+	+	-	-	+	-	+	+	+	-
Melibiose (MEL)	-	+	-	-	+	-	-	+	+	-
Amygdalin (AMY)	-	+	-	-	+	-	-	-	+	-
Arabinose (ARA)	+	+	-	-	+	-	-	+	+	-
Oxidase (OX)	-	-	-	-	-	-	-	-	-	-

Note: ONPG: β-galactosidase test; VP: Acetoin Test; -: negative; +: positive

SEM Images

Figure 3 shows the SEM photos of the above-mentioned samples. It was found that while the cell size varied among the different biofilm-forming bacteria, the majority were rod-shaped.

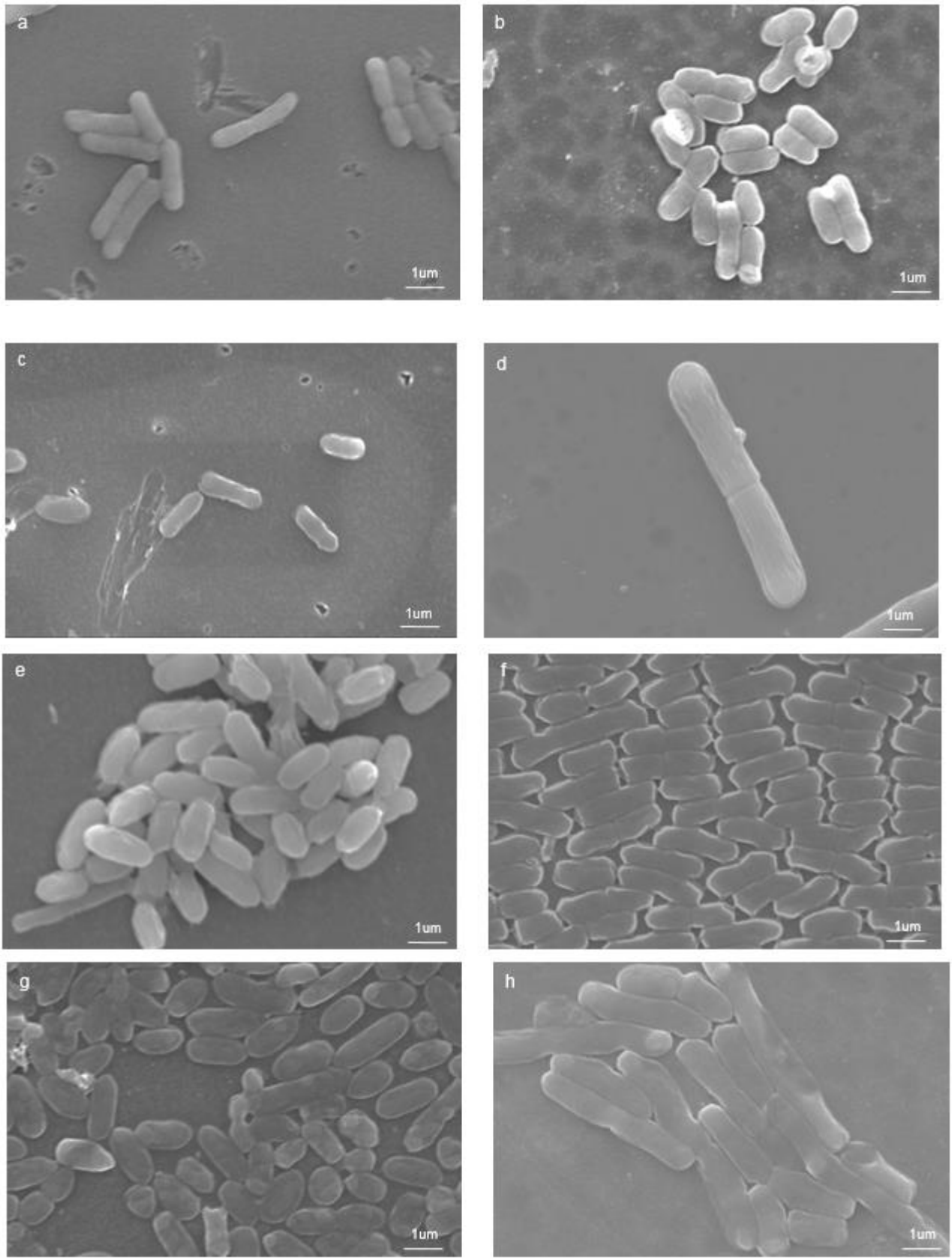

Fig. 3 (a-h). SEM images of the biofilm-forming microorganisms: (a) JLJ12, (b) KB6, (c) KB16, (d) LB24, (e) LB27, (f) NYGA5, (g) NYGA11, (h) NYGA21, (i) NYGA25, and (j) NYGA26

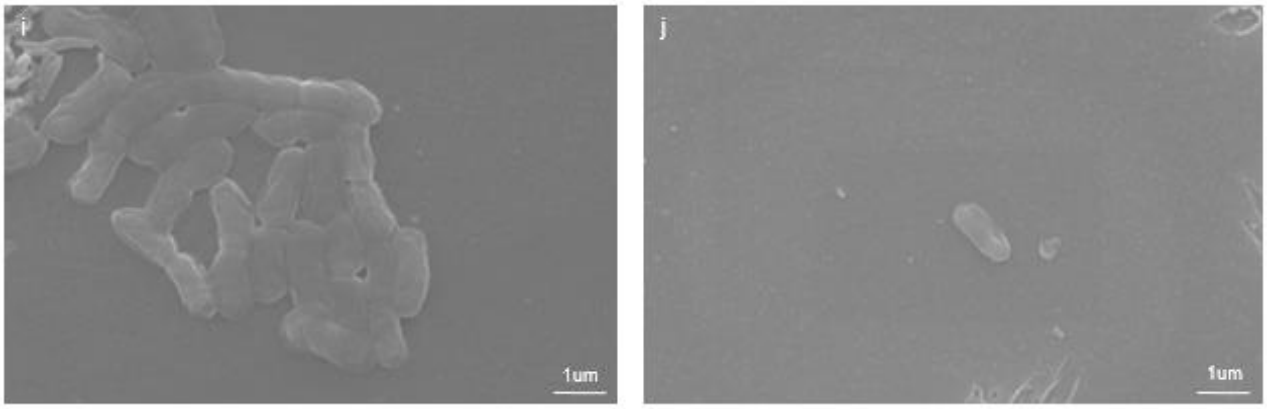

Fig. 3 (i-j). SEM images of the biofilm-forming microorganisms: (a) JLJ12, (b) KB6, (c) KB16, (d) LB24, (e) LB27, (f) NYGA5, (g) NYGA11, (h) NYGA21, (i) NYGA25, and (j) NYGA26

CONCLUSIONS

This paper focuses on the slime problem in the wire section of paper machine using OCC fibers as main material, and discusses the microbial diversity of slime by 16S rDNA and purification. In addition, the biofilm-forming ability of different bacteria was also studied.

1. The sequencing results revealed that the main bacterial phylum in the OCC slime samples was *Proteobacteria*.
2. Among the 99 pure cultures isolated from the slime, the strains *Proteus penneri*, *Klebsiella variicola*, *Klebsiella* sp., and *Proteus mirabilis* all had strong biofilm-forming abilities, and were able to form biofilms on the smooth surface of the test tubes; therefore, these four bacteria should be targeted for removal from slime.

ACKNOWLEDGMENTS

The authors would like to acknowledge the support from the Zhejiang Provincial Natural Science Foundation of China (Grant No. LY15C160002), State Key Laboratory of Pulp and Paper Engineering (Grant No. 201744), Key Research & Development Project of Zhejiang Province (Grant No. 2017C03045), Key Laboratory of Recycling and Eco-treatment of Waste Biomass of Zhejiang Province (Grant Nos. 2016REWB12 and 2016REWB24), Zhejiang Provincial Collaborative Innovation Center of Agricultural Biological Resources Biochemical Manufacturing, and Zhejiang Provincial Key Lab for Chem. & Bio. Processing Technology of Farm Products (Grant Nos. 2016KF0016 and 2016KF0201).

REFERENCES CITED

Ashori, A., Cordeiro, N., Faria, M., and Hamzeh, Y. (2013). "Effect of chitosan and cationic starch on the surface chemistry properties of bagasse paper," *Int. J. Biol. Macromol.* 58, 343-348. DOI: 10.1016/j.ijbiomac.2013.04.056

Barbiroli, A., Bonomi, F., Capretti, G., Iametti, S., Manzoni, M., Piergiovanni, L., and Rollini, M. (2012). "Antimicrobial activity of lysozyme and lactoferrin incorporated in cellulose-based food packaging," *Food Control* 26(2), 387-392. DOI: 10.1016/j.foodcont.2012.01.046

China Paper Association (CPA) (2016). "The annual report of China' paper industry in 2015," *China's Pulp and Paper Industry* 37(11), 20-31.

Chen, H., Chen, K., Yang, R., Yang, F., and Gao, W. (2011). "Use of aluminum trihydrate filler to improve the strength properties of cellulosic paper exposed to high temperature treatment," *BioResources* 6(3), 2399-2410. DOI: 10.15376/biores.6.3.2399-2410

Chen, H., Lou, J., Yang, F., Zhou, J.-N., Zhang, Y., and Yao, H. (2016). "Use of oxalic-acid-modified stellerite for improving the filter capability of $PM_{2.5}$ of paper composed of bamboo residues," *International Journal of Polymer Science* 2016, 1-7. DOI: 10.1155/2016/2198506

Chen, H., Zhang, Y., Wo, Q., Yang, F., Wang, J., Guo, Y., and Zheng, Q. (2015). "Modified PCC used in papermaking processes," *BioResources* (10)3, 5125-5139. DOI: 10.15376/biores.10.3.5125-5139

Dong, C., Li, C., Xiao, H., He, B., and Qian, X. (2014). "β-Cyclodextrin grafted cellulose and cationic starch for antibacterial paper products: A comparative study," *BioResources* 9(2), 3580-3590. DOI: 10.15376/biores.9.2.3580-3590

Fan, H. M., Liu, P., Liu, J. N., and Xu, B. F. (2015). "Effect of hydrodynamic shear on agglomerated ground calcium carbonate filler after surface modification with starch and its effects on paper properties," *BioResources* 10(3), 5655-5665. DOI: 10.15376/biores.10.3.5655-5665

Hettegger, H., Beaumont, M., Potthast, A., and Rosenau, T. (2016). "Aqueous modification of nano- and microfibrillar cellulose with a click synthon," *ChemSusChem* 9(1), 75-79. DOI: 10.1002/cssc.201501358

Li, L., Zhang, M., Song, S., and Wu, Y. (2016a). "Starch/sodium stearate modified fly-ash based calcium silicate: Effect of different modification routes on paper properties," *BioResources* 11(1), 2166-2173. DOI: 10.15376/biores.11.1.2166-2173

Li, T., Fan, J., Chen, W., Shu, J., Qian, X., Wei, H., Wang, Q., and Shen, J. (2016b). "Coaggregation of mineral filler particles and starch granules as a basis for improving filler-fiber interaction in paper production," *Carbohyd. Polym.* 149, 20-27. DOI: 10.1016/j.carbpol.2016.04.082

Lin, Q. B., Wang, T. J., Song, H., and Li, B. (2010). "Analysis of isothiazolinone biocides in paper for food packaging by ultra-high-performance liquid chromatography-tandem mass spectrometry," *Food Addit. Contam.* 27(12), 1775-1781. DOI: 10.1080/19440049.2010.521896

Neyret, C., Herry, J. M., Meylheuc, T., and Dubois-Brissonnet, F. (2014). "Plant-derived compounds as natural antimicrobials to control paper mill biofilms," *J. Ind. Microbiol. Biot.* 41(1), 87-96. DOI: 10.1007/s10295-013-1365-4

Pèlach, M. À., Delgado-Aguilar, M., Alcalá, M., Puig, J., Blanco, Á., and Mutjé, P. (2016). "New strategy for the production of packaging from recycled fibers," *Cell. Chem. Technol.* 50(3-4), 449–454.

Rantanen, J., Dimic-Misic, K., Kuusisto, J., and Maloney, T. (2015). "The effect of micro and nanofibrillated cellulose water uptake on high filler content composite paper properties and furnish dewatering," *Cellulose* 22(6), 4003-4015. DOI: 10.1007/s10570-015-0777-x

Wang, X. B. (2000). "Prevention of slime barrier," *China's Pulp and Paper Industry* 21(3), 42-44.

Article submitted: May 13, 2017; Peer review completed: August 3, 2017; Revised version received and accepted: August 9, 2017; Published: September 6, 2017.
DOI: 10.15376/biores.12.4.7711-7730